

## Electrical Properties of Pulsed Laser Crystallized Silicon Films

Toshiyuki SAMESHIMA, Keiko SAITOH, Naho AOYAMA, Seiichiro HIGASHI<sup>1</sup>,  
Michio KONDO<sup>2</sup> and Akihisa MATSUDA<sup>2</sup>

*Tokyo University of Agriculture & Technology, Tokyo 184-8588, Japan*

<sup>1</sup>*SEIKO Epson Corporation, Nagano 392-8502, Japan*

<sup>2</sup>*Electrotechnical Laboratory, Ibaraki 305-8568, Japan*

(Received October 21, 1998; revised manuscript received December 16, 1998; accepted for publication December 28, 1998)

Electrical properties of phosphorus-doped laser-crystallized silicon films were investigated. The analysis of free carrier optical absorption revealed that crystalline grains formed at laser energies of 360–375 mJ/cm<sup>2</sup> had high carrier mobilities of 40–50 cm<sup>2</sup>/Vs, which were close to that of doped single crystalline silicon. The mobility did not depend on the number of laser pulses. On the other hand, Hall effect measurements showed a marked increase in the carrier mobility of electrical current traversing grain boundaries from 3 to 28 cm<sup>2</sup>/Vs as the laser energy density increased from 160 to 375 mJ/cm<sup>2</sup>. The Hall mobility also increased as the number of laser pulses increased, although a single pulse irradiation resulted in a maximum carrier mobility of 15 cm<sup>2</sup>/Vs. These results suggest that a high laser energy density as well as numbers of multiple pulses are necessary to reduce disordered amorphous states and improve grain boundary properties.

KEYWORDS: optical absorption spectra, free carrier absorption, Hall effect, carrier density, carrier mobility,  $E_2$  peak height

### 1. Introduction

Polycrystalline silicon films are important for a variety of applications in many devices such as thin film transistors (TFTs) and thin film solar cells.<sup>1–10</sup> The electrical properties of polycrystalline silicon films have been analyzed using Hall effect measurements and transistor characteristics. These measurements give the carrier mobility and the density of the carriers which propagate across many grain boundaries in polycrystalline silicon (poly-Si) films. The average energy barrier height at grain boundaries has also been investigated by these methods. We recently reported the possibility of investigating electrical properties of polycrystalline silicon films using free carrier optical absorption analysis.<sup>11,12</sup> Because free carrier optical absorption occurs via excitation induced by the electrical field of incident photons followed by energy relaxation in the crystalline grains, the analysis gives the carrier mobility and the carrier density in the crystalline grains. On the other hand, the Hall effect measurement provides the effective carrier mobility of the electrical current, which traverses many grain boundaries, so it strongly depends on grain boundary properties.

In this paper we discuss electrical properties by analyses of the free carrier optical absorption and Hall effect measurements of pulsed laser crystallized doped silicon films. The pulsed laser crystallization method is convenient to form polycrystalline silicon films at a low processing temperature because of local and rapid heat treatment.<sup>13,14</sup> The method is suitable for fabrication of TFTs and solar cells at a low temperature. Optimization of crystallization, however, has not been achieved. Through the analyses of samples fabricated under different laser-irradiation conditions, we report the relationships between irradiation conditions (laser energy density and pulse number) and electrical properties (carrier mobility and the carrier density). The free carrier optical absorption analysis shows that the doped crystalline grains can have a high average carrier mobility, which is close to that of single crystalline silicon under the same carrier density. The pulse number is important for reduction of the average energy barrier height at grain boundaries and to increase the Hall mobility. We also discuss the crystalline state of the polycrystalline

silicon films by measurements of the  $E_2$  peak which appears in ultraviolet reflectivity spectra.

### 2. Experimental

Doped polycrystalline silicon films 50 nm thick were fabricated by XeCl excimer laser heating of low-pressure chemical vapor deposited (LPCVD) amorphous silicon films on quartz glass substrates. Prior to laser crystallization, phosphorus atoms were uniformly doped into the films through SiO<sub>2</sub> films coated on the silicon films by ion implantation at a density of  $2.5 \times 10^{15}$  cm<sup>-2</sup> and an energy of 80 keV. About 50% phosphorus atoms were doped into the silicon films. After removing the top SiO<sub>2</sub> films, the samples were placed in a vacuum chamber, which was evacuated by a turbo-molecular pump to a level of  $1 \times 10^{-4}$  Pa for laser irradiation. Variation of laser energy density in the beam was reduced to less than 3% of the average laser energy density by beam homogenizing optics. Laser light was effectively absorbed 10 nm deep in the silicon surface because of the large optical absorption coefficient of Si,  $\sim 10^6$  cm<sup>-1</sup>, at 308 nm, and the silicon surface was heated to high temperatures. Above a threshold energy for crystallization of 160 mJ/cm<sup>2</sup>, crystallization occurs by solidification of molten silicon induced by laser irradiation. The solidification (crystallization) velocity was about 1 m/s, which was experimentally determined from the changes in the electrical conductivity of silicon films during and after laser irradiation using transient conductance measurements because liquid silicon has a high electrical conductivity of  $\sim 10^4$  S/cm.<sup>15–17</sup> It has been known that dopant atoms do not segregate from solid to liquid silicon (the segregation coefficient  $\sim 1$ ) under rapid solidification conditions induced by pulsed laser irradiation.<sup>18</sup> We hypothesized that phosphorus atoms were distributed uniformly in crystalline grains and at grain boundaries.

Three kinds of laser irradiation were conducted for sample fabrication. 1) Multiple-step-laser energy irradiation was carried out. Laser energy density was increased from 160 mJ/cm<sup>2</sup> to 400 mJ/cm<sup>2</sup> in 20–40 mJ/cm<sup>2</sup> steps. A single pulse or five pulses were irradiated at each laser energy density step. 2) To investigate the dependence of electrical properties on the number of laser pulses, samples were irradiated

by a laser with pulse numbers from one to twenty at the final laser energy density step. Prior to the final laser energy density step, the laser energy density was increased stepwise with five laser pulse irradiations at each laser energy density step. 3) Samples were also fabricated by laser irradiation with a single pulse at different energies.

The Hall effect measurements by the van der Pauw method were carried out at room temperature for silicon films with an area of 5 mm × 5 mm with Al electrodes formed at each corner to obtain the carrier mobility and the carrier density. The Hall mobility,  $\mu_H$ , is deduced from the relation

$$\mu_H = R_H \sigma = r_H \mu_D \quad (1)$$

$$R = \left| (r_0 + r_1 \exp(i4\pi \tilde{n}_f d K)) (1 + r_0 r_1 \exp(i4\pi \tilde{n}_f d K))^{-1} \right|^2$$

$$r_0 = (1 - \tilde{n}_f) (1 + \tilde{n}_f)^{-1}, \quad r_1 = (\tilde{n}_f - \tilde{n}_{\text{SiO}_2}) (\tilde{n}_f + \tilde{n}_{\text{SiO}_2})^{-1} \quad (2)$$

$$\tilde{n}_f = n_f + ik_f, \quad \tilde{n}_{\text{SiO}_2} = n_{\text{SiO}_2} + ik_{\text{SiO}_2}$$

where  $d$  is the film thickness,  $K$  is the wave number,  $\tilde{n}_f$  and  $\tilde{n}_{\text{SiO}_2}$  are the complex refractive index of Si films and SiO<sub>2</sub> substrate, respectively, which consist of the real refractive indexes ( $n_f$  and  $n_{\text{SiO}_2}$ ) and the extinction coefficients ( $k_f$  and  $k_{\text{SiO}_2}$ ). Undoped crystalline silicon is transparent ( $k_f = 0$ ) in the infrared region. On the other hand, SiO<sub>2</sub> has substantial absorption for wave numbers lower than 2000 cm<sup>-1</sup> so that the reflectivity includes the optical absorption effect of the quartz substrate. A small reflection at the rear surface (air/substrate) was also considered in the calculation of the reflectivity of the samples.

The free carrier optical absorption causes changes in the refractive index as well as in the extinction coefficient, as shown by the following equations;<sup>12,20)</sup>

$$n_f = \frac{1}{\sqrt{2}} \left[ n_{\text{Si}}^2 - A + \left\{ (n_{\text{Si}}^2 - A)^2 + \frac{A^2 e^2}{4\pi^2 m^2 c^2 \mu^2 K^2} \right\}^{0.5} \right]^{0.5}$$

$$k_f = \frac{1}{\sqrt{2}} \left[ A - n_{\text{Si}}^2 + \left\{ (n_{\text{Si}}^2 - A)^2 + \frac{A^2 e^2}{4\pi^2 m^2 c^2 \mu^2 K^2} \right\}^{0.5} \right]^{0.5} \quad (3)$$

$$A = Nm\mu^2\epsilon_0^{-1} (1 + 4\pi^2 m^2 \mu^2 c^2 e^{-2} K^2)^{-1}$$

where  $n_{\text{Si}}$  is the refractive index of undoped crystalline silicon,  $c$  is the velocity of light in vacuum,  $e$  is the electrical charge,  $m$  is the effective mass of the carrier, whose dependence on the carrier density was determined by Miyao *et al.*,<sup>21)</sup>  $K$  is the wave number,  $\mu$  is the carrier mobility, and  $N$  is the carrier density. The experimental spectra were compared to the spectra obtained by the interference calculation given by eq. (1) with the refractive index and the extinction coefficient of silicon given by eq. (2) by changing the values of the parameters of carrier mobility and carrier density until best coincidence of those spectra was obtained.

Optical reflectivity spectra in the ultraviolet region were also measured at the top silicon surface and the bottom silicon/quartz glass interface of the samples. Crystalline silicon has a broad peak around 276 nm ( $E_2$  peak) in optical reflectivity which is caused by a large transition rate at the  $X$  point in the Brillouin zone,<sup>22)</sup> while amorphous silicon has no peak around 276 nm. Because the optical absorption coefficient is large at  $\sim 10^6$  cm<sup>-1</sup> in the ultraviolet region, the crystalline state at the surface and Si/SiO<sub>2</sub> interface regions can be investigated with 10 nm depth resolution. The height of the  $E_2$  peak normalized by the peak reflectivity ( $\Delta R/R$ ) was obtained to estimate crystalline states at both surfaces of the polycrystalline silicon films. The reflectivity spectra at the bottom interface are different from those at the top surface because the refractive index of SiO<sub>2</sub> is larger than that of

where  $R_H$  is the Hall constant,  $\sigma$  is the electrical conductivity,  $r_H$  is the Hall scattering factor and  $\mu_D$  is the drift mobility.

Optical reflectivity was measured in the wave number range between 400 and 4000 cm<sup>-1</sup> by conventional Fourier transform infrared spectrometry (FTIR) to analyze optical absorption of free carriers in the doped silicon films. The sample was irradiated by infrared light with an incidence angle of 10°, and reflection was detected at a resolution of 4 cm<sup>-1</sup>. Reflectivity spectra were analyzed by the optical interference effect at air/Si/substrate. Reflectivity ( $R$ ) at the surface of the air/Si/substrate is given by<sup>19)</sup>

air (= 1). Prior to the determination of  $\Delta R/R$  at the bottom interface, the reflectivity spectra were, therefore, corrected by multiplying a correction factor 0.73, which was obtained by calculations of reflectivity for SiO<sub>2</sub>/Si interfaces with different refractive indexes and extinction coefficients from amorphous to single crystalline silicon to reduce the effect of substrate on the reflectivity.

### 3. Results and Discussion

Figure 1 shows experimental spectra for samples implanted with phosphorus atoms at a density of  $2.5 \times 10^{15}$  cm<sup>-2</sup>, which were fabricated by multiple-step laser energy irradiation with four final laser energies and five laser pulses at each laser energy density step. Although no crystallization of the silicon films and no activation of the phosphorus dopant atoms were observed in the lowest energy irradiation case, the crystallization and the reduction of electrical resistivity associated with dopant activation occurred in the other three cases of higher laser energy density. The reflectivity was reduced in the wave number range from 2000 to 4000 cm<sup>-1</sup> as the laser energy density increased, as shown in Fig. 1. On the other hand, it increased in the wave number range from 500 to 800 cm<sup>-1</sup>. These reflectivity changes resulted from changes in refractive index and extinction coefficient caused by free carrier optical absorption due to activation of the dopant atoms.

Figure 2 shows the calculated reflectivity spectra of 50-

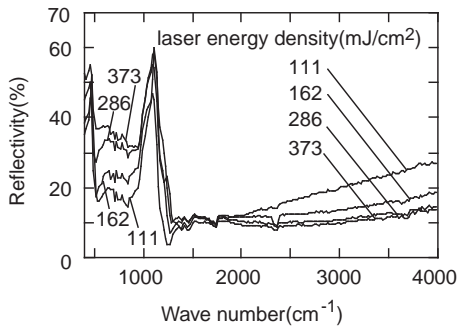
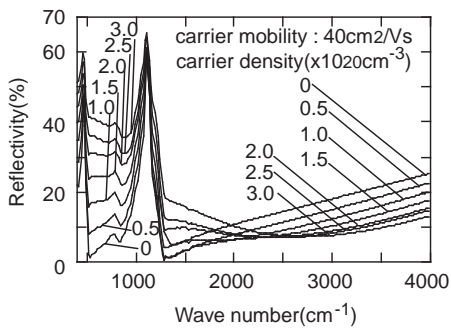
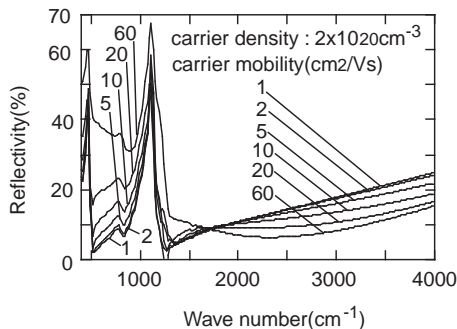


Fig. 1. Experimental reflectivity spectra for 50-nm-thick silicon films implanted with phosphorus atoms at a density of  $2.5 \times 10^{15} \text{ cm}^{-2}$ , which were fabricated by the multiple-step laser energy density irradiation method with four final laser energies and five laser pulses at each laser energy density step. The final laser energy is presented in the figure. The substrate was quartz glass.



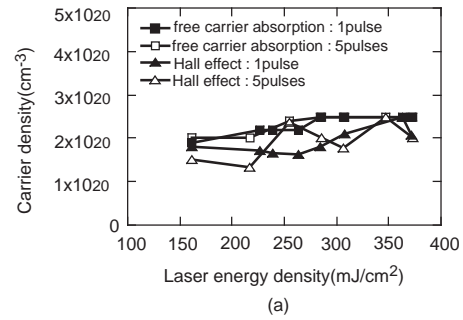
(a)



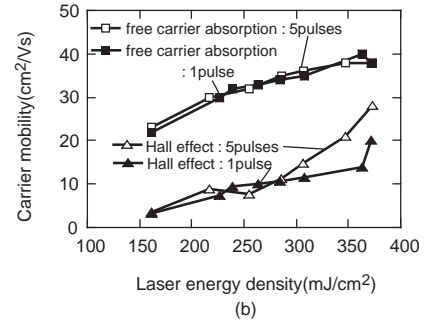
(b)

Fig. 2. Calculated reflectivity spectra of 50-nm-thick silicon/quartz substrates (a) with a carrier mobility of  $40 \text{ cm}^2/\text{Vs}$  and different carrier densities from zero to  $3 \times 10^{20} \text{ cm}^{-3}$ , and (b) with a carrier density of  $2 \times 10^{20} \text{ cm}^{-3}$  and different carrier mobilities from  $1 \text{ cm}^2/\text{Vs}$  to  $60 \text{ cm}^2/\text{Vs}$ .

nm-thick silicon/quartz substrates using eqs. (2) and (3) with a carrier mobility of  $40 \text{ cm}^2/\text{Vs}$  and different carrier densities from zero to  $3 \times 10^{20} \text{ cm}^{-3}$  [Fig. 2(a)], and with a carrier density of  $2 \times 10^{20} \text{ cm}^{-3}$  and different carrier mobilities from  $1$  to  $60 \text{ cm}^2/\text{Vs}$  [Fig. 2(b)]. The low carrier density and the low carrier mobility resulted in a monotonous increase in the reflectivity with increasing wave number from  $1300$  to  $4000 \text{ cm}^{-1}$  and a low reflectivity at wave numbers between  $500$  and  $800 \text{ cm}^{-1}$ . Reduction in the reflectivity was observed for wave numbers between  $1300$  and  $4000 \text{ cm}^{-1}$  as the carrier density and carrier mobility increased because the substantial free carrier optical absorption reduced the refractive index of silicon films ( $n_f$ ). On the other hand, the reflectivity increased for wave numbers between  $500$  and  $800 \text{ cm}^{-1}$  as the



(a)



(b)

Fig. 3. (a) Carrier density and (b) carrier mobility obtained by analyses of free carrier optical absorption and by Hall effect measurements with the assumption of a Hall scattering factor of unity for phosphorus-doped 50-nm-thick silicon films crystallized by laser irradiation, by increasing the laser energy density stepwise with one pulse and five pulses at each laser energy density step.

carrier density and carrier mobility increased because the free carrier optical absorption causes an increase in the extinction coefficient of the silicon films ( $k_f$ ) in that wave number range. Because the dependence of the refractive index or the extinction coefficient on the carrier density and the carrier mobility differs as shown in eq. (3), the calculation of reflectivity spectra most similar to experimental ones gives the carrier density and the carrier mobility.

Figure 3 shows (a) the carrier density and (b) the carrier mobility obtained by analyses of free carrier optical absorption with best coincident fitting of calculated reflectivity spectra to experimental spectra for samples crystallized by laser irradiation by increasing the laser energy density stepwise one and five pulses at each laser energy density step. Figure 3 also shows (a) the carrier density and (b) the carrier mobility obtained by Hall effect measurements when the Hall scattering factor was assumed to be equal to unity. Both analyses of free carrier optical absorption and Hall effect gave approximately the same carrier density, as shown in Fig. 3(a). The carrier density was slightly increased to  $2.5 \times 10^{20} \text{ cm}^{-3}$  as the laser energy density increased from  $160$  to  $280 \text{ mJ/cm}^2$ , and it leveled off at laser energy densities higher than  $280 \text{ mJ/cm}^2$ . Dopant atoms were effectively activated and a high density of carriers was generated. An increase in carrier density with increasing laser energy density probably means that the activation was not completed over the entire film thickness in the low laser energy density region. The analysis of free carrier optical absorption gave a large carrier mobility about  $20 \text{ cm}^2/\text{Vs}$  at laser energy densities immediately above the crystallization threshold. The carrier mobility increased to  $40 \text{ cm}^2/\text{Vs}$  as the laser energy density increased. Irradiation with a single pulse and five pulses at each laser energy density step resulted in approximately the same carrier mobilities.

These results indicate that laser irradiation led to the formation of crystalline grains with good electrical characteristics even for lower laser energy densities near the crystallization threshold, although transmission electron microscopy (TEM) revealed that very fine crystalline grains with an average size of about 10 nm were formed by laser irradiation at the laser energy density of the crystallization threshold.<sup>23)</sup> A gradual increase in the carrier mobility with increasing laser energy density probably resulted from the improvement of the crystalline properties; such as an increase in the average grain size or a reduction in the density of defect states. On the other hand, no change in the carrier mobility with number of laser pulses means that the number of laser pulses did not play an important role in the improvement of crystalline grain properties. The Hall effect measurements resulted in lower carrier mobilities than those obtained by the free carrier optical absorption analysis especially for samples treated with low laser energy densities. The carrier mobility obtained by the Hall effect measurements markedly increased as the laser energy density increased from 3 to 28 cm<sup>2</sup>/Vs. The degree of increase in carrier mobility obtained by Hall effect measurements was much larger than that obtained by the free carrier optical absorption analysis. This large increase is interpreted as improvement in the grain boundary properties by laser irradiation with a high energy density, because the Hall mobility strongly depends on carrier trap states and a high potential energy barrier height at grain boundaries. Disordered states with a high density of dangling bonds at grain boundaries are reduced by high-energy irradiation because of the long melt duration and the low quenching rate. Moreover, the carrier mobility obtained by Hall effect measurements for samples crystallized with five pulses at each laser energy density step was higher than that for samples crystallized with single pulses at each laser energy density step for high final laser energy densities of 300–375 mJ/cm<sup>2</sup>.

Figure 4 gives the carrier mobility as a function of the number of laser pulses from one to twenty at a final laser energy density of 360 mJ/cm<sup>2</sup>. Prior to the final laser energy density, five laser pulses were irradiated at each laser energy density step. Although the carrier mobility obtained by free carrier optical absorption analysis was 50 cm<sup>2</sup>/Vs, which did not depend on the number of laser pulses, the carrier mobility obtained by Hall effect measurements increased from 15 to 25 mJ/cm<sup>2</sup> as the laser pulse number increased. This means that irradiation with multiple laser pulses is important to im-

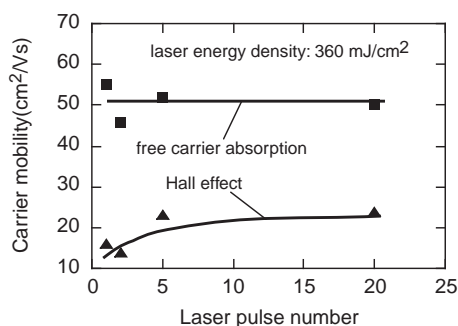


Fig. 4. Carrier mobilities obtained by analyses of free carrier absorption and by Hall effect measurements assuming a Hall scattering factor of unity as a function of number of pulses at a final energy density of 360 mJ/cm<sup>2</sup> in the method of multiple-step laser energy density irradiation.

prove electrical properties at grain boundaries; the reformation of grain boundaries through melting followed by solidification might effectively reduce the density of carrier trap states and energy barrier heights. The maximum carrier mobility,  $\sim 50$  cm<sup>2</sup>/Vs, obtained by analysis of free carrier optical absorption was close to that of single crystalline doped silicon given by Irvin.<sup>24)</sup> The crystalline grains have approximately the same electrical properties as doped single crystalline silicon.

The crystalline state was investigated by measuring heights of the normalized  $E_2$  peaks ( $\Delta R/R$ ) at the top surface and the bottom interface for samples crystallized by laser irradiation by increasing the laser energy density stepwise with five pulses at each laser energy density step; the carrier density and carrier mobility are presented in Fig. 3. A small  $E_2$  peak was observed at both surfaces of silicon films for energies higher than the threshold energy. Low normalized  $E_2$  peak height for irradiation at low laser energy density means that there are serious disordered amorphous states among the crystalline grains. The normalized  $E_2$  peak heights ( $\Delta R/R$ ) at both surfaces increased as the laser energy density increased. The crystallization occurred throughout the film thickness for energies immediately above the threshold energy density, and the crystalline volume fraction increased as the laser energy density increased. The normalized heights of the  $E_2$  peak at the top surface were almost the same as the normalized height of the  $E_2$  peak of single crystalline silicon for laser energy densities higher than 320 mJ/cm<sup>2</sup>. The crystalline state is dominant at the top surface region for those conditions of high energy density.

Changes in the heights of the  $E_2$  peaks with the laser energy density correlated well with changes in the carrier mobility obtained by the analysis of free carrier optical absorption with the laser energy density, as shown in Figs. 3 and 5. The improvement in crystalline state results in high carrier mobility. However, the normalized heights of the  $E_2$  peaks did not change substantially for laser energy densities above 320 mJ/cm<sup>2</sup>, while there was a marked increase in the Hall mobility with increasing laser energy densities above 320 mJ/cm<sup>2</sup>. Irradiation with high laser energy densities increased crystalline grain size and induced the formation of grain boundaries with almost zero thickness among crystalline grains with different orientation angles, as TEM observations suggested.<sup>9, 10, 25)</sup> Moreover, irradiation with high laser energy densities and multiple pulses reduces the densi-

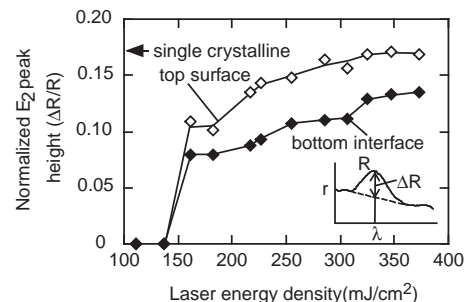


Fig. 5.  $E_2$  peak heights normalized by the peak reflectivity ( $\Delta R/R$ ) at the top surface and the bottom interface for phosphorus-doped 50-nm-thick silicon films crystallized by laser irradiation by increasing the laser energy density stepwise with five pulses at each energy density step. The normalized  $E_2$  peak height of single crystalline silicon, 0.172, is also shown.

ties of dangling bonds and weak bonds and reduces the average energy barrier heights via the formation of stable grain boundaries such as the coincident boundaries of the lattice sites that are electrically inactive, as suggested by various observations and theoretical calculations.<sup>26–28</sup>) Defect states and potential energy barrier heights at grain boundaries can cause scattering of carriers and reduce the Hall scattering factor to be lower than unity. Although the Hall scattering factor was not determined in this study, Shirai and Serikawa reported a Hall scattering factor of 0.87 for laser crystallized silicon films, which was estimated experimentally from the Hall mobility and the field effect mobility of poly-Si TFTs.<sup>29</sup>) Because similar field effect mobilities to that of Shirai and Serikawa's TFTs was obtained for TFTs fabricated in poly-Si films by pulsed XeCl excimer laser irradiation with high laser energy densities near the amorphization threshold,<sup>5</sup>) we deduce that the drift mobility was about 10% higher than the Hall mobility shown in Figs. 3 and 4 for cases of irradiation with high laser energy densities ( $> 300 \text{ mJ/cm}^2$ ). Because Le Bihan *et al.* reported a Hall scattering factor of 0.65 for solid phase crystallized silicon films with a higher density of trap states at grain boundaries than that of Shirai and Serikawa's laser crystallized silicon films,<sup>30</sup>) the Hall scattering factor might be lower than 0.87 for irradiation with lower laser energy densities near the crystallization threshold. According to this discussion, the average energy barrier height at grain boundaries ( $\Delta E$ ) can be roughly estimated by assuming a simple relation between the drift mobility and the carrier mobility in crystalline grains,  $\mu_D = r_H^{-1} \times \mu_H = \mu_A \exp(-\Delta E/kT)$ , where  $\mu_A$ ,  $k$  and  $T$  are the average carrier mobility in crystalline grains obtained by the free carrier optical absorption, the Boltzmann constant and the absolute temperature, respectively. The minimum average energy barrier height was 11 meV under these laser irradiation conditions when the maximum average carrier mobility in crystalline grains, the maximum average Hall mobility and the Hall scattering factor were  $50 \text{ cm}^2/\text{Vs}$ ,  $28 \text{ cm}^2/\text{Vs}$  and 0.87, respectively.

Figure 6 shows (a) the carrier density and (b) the carrier mobility for samples crystallized by laser irradiation with only one pulse. Both the analyses of free carrier optical absorption and Hall effect measurements assuming a Hall scattering factor of unity gave approximately the same carrier density,  $1.7\text{--}2.5 \times 10^{20} \text{ cm}^{-3}$ , for each laser energy density. The phosphorus atoms were effectively activated by a single laser pulse for laser energy densities from 165 to  $400 \text{ mJ/cm}^2$ . The carrier mobility obtained by free carrier optical absorption analysis was larger than that obtained by Hall effect measurements. It had a maximum value of  $38 \text{ cm}^2/\text{Vs}$  at laser energy densities of  $260\text{--}300 \text{ mJ/cm}^2$ , which was approximately the same as the maximum mobility resulting from multiple-laser-pulse crystallization, as shown in Fig. 3. The high-quality crystalline grains are formed by annealing with a single laser pulse. On the other hand, the maximum Hall mobility was  $15 \text{ cm}^2/\text{Vs}$ , which was lower than the maximum carrier mobility for multiple-pulse irradiation. Single laser irradiation might not be sufficient to form a grain boundary with a low energy barrier. Carrier mobility decreased as the laser energy density increased from 280 to  $400 \text{ mJ/cm}^2$  in contrast to the monotonous increase in the carrier mobility in the multiple-laser-pulse crystallization case, as shown in Figs. 3 and 6.

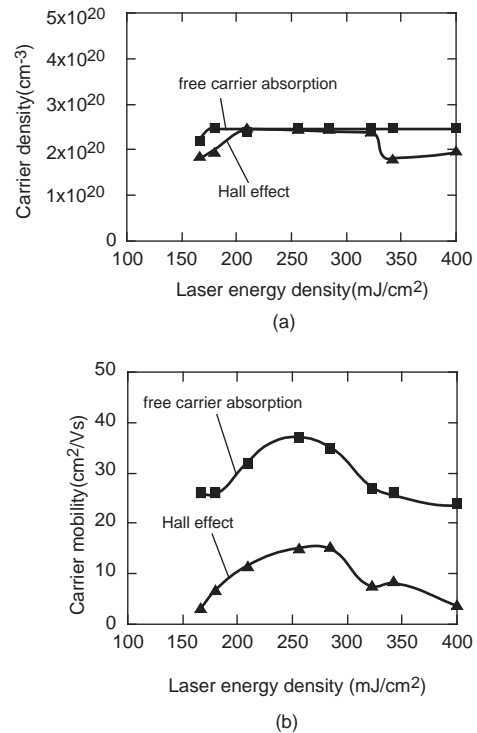


Fig. 6. (a) Carrier density and (b) carrier mobility obtained by analyses of free carrier optical absorption and by Hall effect measurements assuming a Hall scattering factor of unity for phosphorus-doped 50-nm-thick silicon films crystallized by laser irradiation with only one pulse.

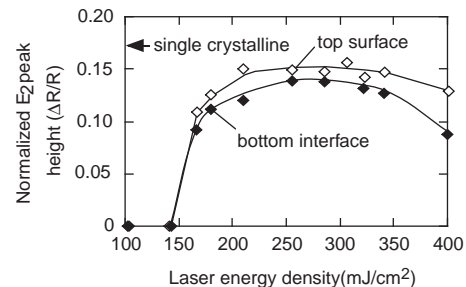


Fig. 7.  $E_2$  peak heights normalized by the peak reflectivity ( $\Delta R/R$ ) at the top surface and the bottom interface for phosphorus-doped 50-nm-thick silicon films crystallized by laser irradiation with only one pulse.

The  $E_2$  peak heights normalized by the peak reflectivity ( $\Delta R/R$ ) at the top surface and the bottom interface were also measured for the single pulse crystallization case, and the results are shown in Fig. 7. The normalized  $E_2$  peak heights at the both silicon surfaces increased as the laser energy density increased above the crystallization threshold, and reached a maximum at laser energy densities of  $260\text{--}300 \text{ mJ/cm}^2$ , which were coincident energy densities that gave a maximum value for carrier mobility, as shown in Fig. 6. The maximum value of the normalized peak heights ( $\Delta R/R$ ) at both silicon surfaces was close to that of single crystalline silicon. The 50-nm-thick amorphous silicon films were crystallized entirely by a single laser pulse at laser energy densities of  $260\text{--}300 \text{ mJ/cm}^2$ . The normalized heights of  $E_2$  peak at both silicon surfaces decreased as the laser energy density increased above  $300 \text{ mJ/cm}^2$ . Disordered amorphous states are formed substantially above  $300 \text{ mJ/cm}^2$ . The normalized heights of  $E_2$  peak at the bottom interface decreased

to smaller values than that at the top surface. The decrease in the carrier mobility and the normalized heights of  $E_2$  peak with increasing laser energy density above 280 mJ/cm<sup>2</sup> shown in Figs. 6 and 7 was probably caused by microcrystallization,<sup>31)</sup> which occurs through rapid solidification of deep-undercooled molten silicon induced by complete melting of the silicon films. Very small ~10 nm crystalline grains are formed through rapid crystallization, and disordered amorphous states are also formed. The microcrystalline state would dominate at the bottom interface because of small normalized  $E_2$  peak heights at the bottom surface. Because amorphous silicon has a higher internal energy and a lower melting point than crystalline silicon, single pulse irradiation can melt a silicon film completely at lower laser energy densities compared with multiple-laser-pulse crystallization, which changes the films from amorphous to crystalline during the stepwise increase of laser energy density. Microcrystallization was not observed for laser energy densities lower than 400 mJ/cm<sup>2</sup> in multiple-laser-pulse crystallization, as shown in Figs. 3 and 5.

#### 4. Summary

The electrical properties of phosphorus-doped pulsed laser crystallized silicon films were investigated by analyses of free carrier optical absorption and Hall effect measurements. The analysis of free carrier optical absorption revealed that the carrier mobility increased from 20 to 40 cm<sup>2</sup>/Vs as the laser energy density increased from 160 to 375 mJ/cm<sup>2</sup> by XeCl excimer laser irradiation by increasing the laser energy density stepwise in vacuum for silicon films 50 nm thick implanted with phosphorus atoms at a density of  $2.5 \times 10^{15}$  cm<sup>-2</sup>. The mobility did not depend on number of laser pulses, and its maximum was close to that of doped single crystalline silicon. On the other hand, the carrier mobility obtained by Hall effect measurements markedly increased from 3 to 28 cm<sup>2</sup>/Vs as the laser energy density increased or the number of laser pulses increased. The  $E_2$  peak height normalized by the peak reflectivity ( $\Delta R/R$ ) at the top silicon surface and the bottom Si/substrate interface increased as the laser energy density increased. From these results, we interpret that crystalline grains formed by irradiation at laser energy densities above the crystallization threshold have good properties and high carrier mobility, but high laser energy densities as well as numbers of multiple pulses are required to reduce disordered amorphous states and improve grain boundary properties to increase the carrier mobility of electrical current traversing through grain boundaries. The energy barrier height was estimated to be 11 meV from the difference in the maximum mobilities obtained by these two methods. Single pulse irradiation caused crystallization of doped silicon films entirely, but the maximum carrier mobility was 15 cm<sup>2</sup>/Vs, which was lower than that obtained by multiple-pulse irradiation. In the case of single pulse irradiation, degradation of the crystalline state and reduction of carrier mobility probably caused by

microcrystallization were observed for laser energy densities from 300–400 mJ/cm<sup>2</sup>, which were realized under cooling because of the low melting point of initial amorphous silicon.

#### Acknowledgements

The authors would like to thank H. Oshima, S. Inoue, T. Saitoh and T. Mohri for their support.

- 1) T. Sameshima, S. Usui and M. Sekiya: IEEE Electron Device. Lett. **7** (1986) 276.
- 2) K. Sera, F. Okumura, H. Uchida, S. Itoh, S. Kaneko and K. Hotta: IEEE Trans. Electron Devices **36** (1989) 2868.
- 3) T. Serikawa, S. Shirai, A. Okamoto and S. Suyama: Jpn. J. Appl. Phys. **28** (1989) L1871.
- 4) H. Kuriyama, T. Kuwahara, S. Ishida, T. Nohda, K. Sano, H. Iwata, S. Noguchi, S. Kiyama, S. Tsuda, S. Nakano, M. Osumi and Y. Kuwano: Jpn. J. Appl. Phys. **31** (1992) 4550.
- 5) A. Kohno, T. Sameshima, N. Sano, M. Sekiya and M. Hara: IEEE Trans. Electron Devices **42** (1995) 251.
- 6) M. Miyasaka, T. Komatsu, A. Shimodaira, I. Yudasaka and H. Ohshima: Jpn. J. Appl. Phys. **34** (1995) 921.
- 7) A. Matsuda: J. Non-Cryst. Solids **56–60** (1983) 767.
- 8) Y. Chida, M. Kondo and A. Matsuda: J. Non-Cryst. Solids **198–200** (1996) 1121.
- 9) E. Fogarassy, B. Prevot, S. De Unamuno, E. Ellici, H. Pattyn, E. L. Mathe and A. Naudon: Appl. Phys. A **56** (1993) 365.
- 10) P. Mei, J. B. Boyce, M. Hack, R. A. Lujan, R. I. Johnson, G. B. Anderson, D. K. Fork and S. E. Ready: Appl. Phys. Lett. **64** (1994) 1132.
- 11) T. Sameshima, N. Takashima, K. Saitoh and N. Betsuda: *Proc. Third Symp. Thin Film Transistor Technologies*, ed. Y. Kuo (Electrochemical Society, Pennington, New Jersey, 1996) Vol. 96-23, p. 296.
- 12) T. Sameshima, K. Saitoh, M. Satoh, A. Tajima and N. Takashima: Jpn. J. Appl. Phys. **36** (1997) L1360.
- 13) D. H. Lowndes, G. E. Jellison, Jr. and R. F. Wood: Phys. Rev. B **26** (1982) 6747.
- 14) T. Sameshima, M. Hara and S. Usui: Jpn. J. Appl. Phys. **28** (1989) L2131.
- 15) G. J. Galvin, M. O. Thompson, J. W. Mayer, R. B. Hammond, N. Paulter and P. S. Peercy: Phys. Rev. Lett. **48** (1982) 33.
- 16) V. M. Glazov, S. N. Chizhenskaya and N. N. Glagoleva: *Liquid Semiconductor* (Plenum Press, New York, 1969) p. 60.
- 17) T. Sameshima, M. Hara and S. Usui: Jpn. J. Appl. Phys. **28** (1989) 1789.
- 18) R. F. Wood, J. R. Kirkpatrick and G. E. Giles: Phys. Rev. B **23** (1981) 5555.
- 19) M. Born and E. Wolf: *Principles of Optics* (Pergamon, New York, 1974) Chaps. 1 and 13.
- 20) H. Engstrom: J. Appl. Phys. **51** (1980) 5245.
- 21) M. Miyao, T. Motooda, N. Natuaki and T. Tokuyama: *Proceeding in Laser and Electron-Beam Solid Interactions and Materials Processing* (Elsevier, North Holland, Amsterdam, 1981) p. 163.
- 22) J. R. Chelikowsky and M. L. Cohen: Phys. Rev. B **10** (1974) 5095.
- 23) T. Sameshima and S. Usui: Mater. Res. Soc. Symp. Proc. **71** (1986) 435.
- 24) J. C. Irvin: Bell Syst. Tech. J. **41** (1962) 387.
- 25) J. S. Im, H. J. Kim and M. O. Thompson: Appl. Phys. Lett. **63** (1993) 1969.
- 26) A. Bourret and J. J. Bacmann: Surf. Sci. **162** (1985) 495.
- 27) A. T. Paxton and A. P. Sutton: J. Phys. C **21** (1988) L481.
- 28) M. Koyama, R. Yamamoto, R. Ebata and M. Kinoshita: J. Phys. C **21** (1988) 3205.
- 29) S. Shirai and T. Serikawa: IEEE Trans. Electron Devices **39** (1992) 450.
- 30) F. Le Bihan, B. Fortin, H. Lhermite, O. Bonnaud and D. Briand: *Poly-crystalline Semiconductors III*, eds H. P. Strunk, J. H. Werner, B. Fortin and O. Bonnaud (Scitec Publications, Zuerich-Uetikon, 1994) p. 379.
- 31) T. Sameshima and S. Usui: Appl. Phys. Lett. **59** (1991) 2724.